

Cation distribution and magnetization of $\text{BaFe}_{12-2x}\text{Co}_x\text{Sn}_x\text{O}_{19}$ ($x=0.9, 1.28$) single crystals

Felip Sandiumenge and Benjamín Martínez

ICMAB-CSIC Campus Universitari de la UAB. 08193 Bellaterra, Spain

Xavier Batlle

Departament de Física Fonamental, UB. Av. Diagonal 647, 08028 Barcelona, Spain

Salvador Galí

Departament de Cristal·lografia, UB. C/ Martí i Franquès S/N. 08028 Barcelona, Spain

Xavier Obradors

ICMAB-CSIC Campus Universitari de la UAB. 08193 Bellaterra, Spain

(Received 28 April 1992; accepted for publication 4 August 1992)

The distribution of Sn^{4+} cations within the five crystallographic sites of the magnetoplumbite (M)-like compound $\text{BaFe}_{12-2x}\text{Co}_x\text{Sn}_x\text{O}_{19}$ has been analyzed using single-crystal x-ray-diffraction data. The species Fe^{3+} and Co^{2+} cannot be distinguished using x rays because of their very similar atomic numbers; however, the calculation of the apparent valencies for the different sites allows an insight into the Co^{2+} cation segregation. The use of previous data from neutron powder diffraction allows a precise picture of the cation distribution, which indicates a pronounced site selectivity for both Sn^{4+} and Co^{2+} cations. The Sn^{4+} cations prefer the $4f_2$ sites and to a much lower extent the $12k$ sites, while they do not enter the octahedral $2a$ sites at all. Co^{2+} cations are distributed among tetrahedral and octahedral sites displaying a clear preference for the tetrahedral $4f_1$ sites. Magnetic measurements indicate that the compound still exhibits uniaxial anisotropy with the easy direction parallel to the c axis. Nevertheless, the magnetic structure shows a considerable degree of noncolinearity. A strong reduction of the magnetic anisotropy regarding that of the undoped compound is also detected.

I. INTRODUCTION

Hexagonal ferrites are a large family of hexagonal or rhombohedral ferrimagnetic oxides with interesting properties as permanent magnets, microwave device materials, and magnetic and magneto-optic recording media,¹ so that many efforts have been devoted to adjusting their magnetic properties by cation substitutions.² The M (magnetoplumbite)³-type $\text{BaFe}_{12}\text{O}_{19}$ (Ref. 4) compound has been largely investigated. Its crystal structure (SG $P6_3/mmc$) is symbolically described as a $\dots RSR^*S^*\dots$ c -stacked sequence, where the R block contains three layers (two O_4 and one BaO_3) and has the composition $(\text{BaFe}_6\text{O}_{11})^{2-}$, and S is a two O_4 layer block which is a (111) slice of the cubic spinel structure with the $\langle 111 \rangle_{\text{cubic}}$ direction parallel to the hexagonal c axis, and has the composition $(\text{Fe}_6\text{O}_8)^{2+}$. The asterisk indicates that the corresponding block has been rotated 180° around the hexagonal axis. The metallic cations are distributed among five different crystallographic sites, namely, three octahedral ($2a$, $12k$, and $4f_2$), one tetrahedral ($4f_1$), and one trigonal dipyramidal environment where the cation is disordered between two adjacent pseudotetrahedral sites [$4e(\frac{1}{2})$]. In the pure M-type $\text{BaFe}_{12}\text{O}_{19}$ compound, the ferric cation placed in this site suffers a fast diffusional motion between the two equivalent pseudotetrahedral sites, separated by $0.340(1)$ Å.⁴ The content of the unit cell is displayed in Fig. 1.

The pure M-type compound, $\text{BaFe}_{12}\text{O}_{19}$, is ferrimagnetic below $T_c \sim 720$ K.^{5,6} In the magnetic structure proposed by Gorter,⁵ all the magnetic moments of the ferric

cations are aligned with the hexagonal c axis, those located in $2a$, $4e(\frac{1}{2})$, and $12k$ being opposed to those located in $4f_1$ and $4f_2$ crystallographic sites. The crystal structure (see Fig. 1) is composed by 2D layers of edge sharing octahedra ($12k$ sites) lying on the R - S interphases, and are connected one to each other either through the face-sharing octahedra ($4f_2$ sites) and the dipyramids, in the R block, or through the octahedra ($2a$ sites) and tetrahedra ($4f_1$ sites) in the S block. Isalgúe *et al.*⁷ reported that the ferric cations located in the face-sharing $4f_2$ octahedra are actually an important superexchange path within the structure, while for the $12k$ edge-sharing octahedra strongly competing interactions induce a low stability of the spin arrangement. Therefore, in substituted isomorphs, the stability of the colinear spin arrangement will depend to a large extent on selective dilution effects. In particular, the preferential occupation of the $4f_2$ sites by Ti^{4+} diamagnetic cations in $\text{BaFe}_{12-2x}\text{Co}_x\text{Ti}_x\text{O}_{19}$ induces a wide variety of magnetic behaviors as a function of the doping rate, evolving from ferrimagnetic to a spin glass state for $x=6$.⁸

The M-type $\text{BaFe}_{12}\text{O}_{19}$ is especially important as perpendicular recording media and many substitutions involving Co^{2+} , in order to decrease its high intrinsic magnetocrystalline anisotropy, have been attempted.⁹ Charge compensation requires the substitution scheme $\text{BaFe}_{12-2x}\text{Co}_x^{2+}\text{M}_x^{4+}\text{O}_{19}$, where $\text{M}^{4+}=\text{Ti}^{4+}$ has been widely investigated.¹⁰ However, $\text{M}^{4+}=\text{Sn}^{4+}$ has been shown to be an interesting alternative since similar decreases of the coercive field can be achieved at lower substitution rates.¹¹ Therefore, the influence of the Co^{2+} dia-

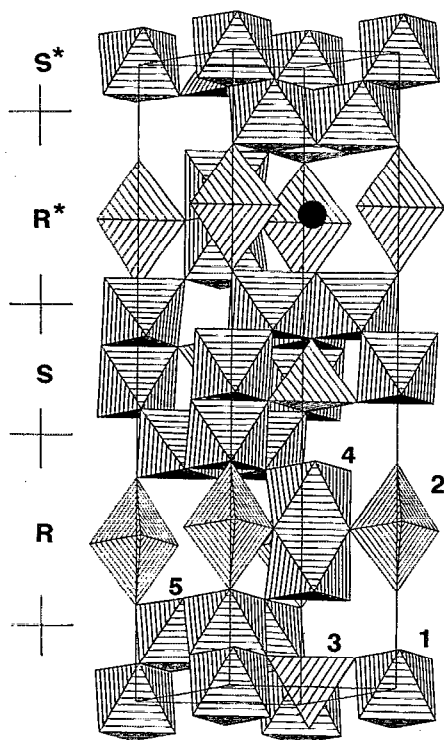


FIG. 1. Polyhedral representation of the content of the unit cell of the magnetoplumbite-type structure. The different crystallographic sites are numbered according to Table I.

magnetic companion cation appears to be of great interest. Up to now, studies on cation distribution of Co–Sn–Fe-containing M-type compounds have used powder neutron diffraction.¹² However, this technique cannot give a unequivocal determination of the site occupancies of the three different species within the five different crystallographic sites. Alternatively, owing to the very similar atomic numbers of Co and Fe, x-ray diffraction allows the univocal determination of Sn site occupancies. Hence, x rays and neutrons appear to be two useful complementary tools for the precise determination of the cation distribution in this particular system.

In this article, we report an x-ray-diffraction study of a $\text{BaFe}_{12-2x}\text{Co}_x\text{Sn}_x\text{O}_{19}$ ($x=1.28$) single crystal. The results match well with the previous observations using neutron powder diffraction.^{12,13} In addition, the analysis of the apparent valencies¹⁴ for the different crystallographic sites are proved to give a useful insight into the possible location of Co^{2+} cations.

II. EXPERIMENT

A. Sample preparation

Two different compositions were used for the present study, both obtained by slow cooling of $\text{BaO}\cdot\text{B}_2\text{O}_3$ fluxed melts.¹⁵ First, a mixture (in mol %) of 42.5 BaO, 29.4 BaO, 24.1 Fe_2O_3 , 2.0 CoO, and 2.0 SnO_2 was melted in a 30 cm³ platinum crucible up to 1290 or 1300 °C and slowly cooled at 3 °C·h⁻¹ to 1000 °C. Crystals with an unusual habit consisting of large dipyramidal $\{10\bar{1}1\}$, $\{10\bar{1}2\}$, and

$\{10\bar{1}3\}$ forms, and almost absent basal $\{0001\}$ faces,¹⁶ and measuring up to 3 mm along $\langle 001 \rangle$, were obtained. Second, a mixture (in mol %) of 42.5 BaO, 29.4 BaO, 20.1 Fe_2O_3 , 4.0 CoO, and 4.0 SnO_2 , was melted in a 30 cm³ platinum crucible at 1290 or 1300 °C, and slowly cooled at 0.8 °C h⁻¹ to 1152 °C. In this case, single crystals displaying the usual habit of magnetoplumbites, i.e., plate-shaped crystals, with maximum size 3 mm in diameter and 1.5 mm in height were obtained. BaCO_3 and Co_3O_4 were used for BaO and CoO, respectively; all were Merck pro analysis chemicals. In all the batches, an initial charge of the starting components weighing 60 g was used. The crystals were separated from the residual solidified flux by dissolution in hot diluted HNO_3 . The average chemical composition, deduced by EDAX-ZAF (Ref. 17) performed on several crystallites, indicated a stoichiometric coefficient, $x=0.9$ and 1.4 for the crystals obtained in the first and second experiments, respectively. Metallic Fe, Co, and Sn, and BaSO_4 were used as standards (provided by C. M. Taylor Corp.). A certain degree of compositional dispersion within the crystals obtained in one single batch was observed. This phenomenon is difficult to avoid in unstirred viscous solutions. Moreover, EDX analyses performed on polished crystal slices indicated compositional homogeneity within experimental accuracy. The magnetoplumbite structure (S. G. $P6_3/mmc$, $Z=2$) was confirmed by inspection of $hh\text{-}2hl$ and $hki0$ heavily exposed precession photographs using small cleavage fragments.

B. Structure

For the diffractometer measurements, crystals of the second experiment were used in order to obtain a more obvious picture of the Sn distribution. A group of cleavage fragments were polished to spheres. A single-crystal sphere with radius $R=0.014$ cm was selected and mounted on an Enraf Nonius CAD-4 diffractometer with graphite monochromated $\text{MoK}\alpha$ radiation. The cell parameters calculated using 25 centered reflections in the angular range $16^\circ < 2\theta < 38^\circ$ were $a=b=5.9341(2)$ Å and $c=23.4845(33)$ Å. A total of 2657 reflections were measured within $1^\circ < \theta < 25^\circ$, $-7 < h, k < 7$, and $0 < l < 27$ in a $\omega-2\theta$ scan mode. Intensities were corrected for Lorentz polarization factor, and spherical absorption ($\mu R=2.12$) was accounted for by fitting the variation of the transmittance with θ through the $A^*(\theta)$ values available in Ref. 18. After averaging in the $6/mmm$ Laue class 289 unique reflections were obtained, of which 254 with $F_0 < 3\sigma(F_0)$ were used for the calculations. The refinement was carried out with the SHELX-76 program.¹⁹ Because of the very similar atomic numbers of Co and Fe, the scattering factor of Fe was used for $M=\text{Fe}+\text{Co}$. This procedure allows the unequivocal determination of the Sn site occupancies. In order to keep the ratio of the number of observed reflections to the number of variables as low as possible, anisotropic temperature coefficients were only included for Ba, M2, and (Sn,M)4 atoms [$2d$, $4e(\frac{1}{2})$ and $4f_2$ sites, respectively], because the first is the heaviest cation, and the latter two presented a fairly distorted electron density distribution. By inspection of difference Fourier maps, it was

TABLE I. Fractional coordinates, site occupation factors (SOF), and thermal parameters for $\text{BaFe}_{12-2x}\text{Co}_x\text{Sn}_x\text{O}_{19}$ ($x=1.28$). $M=\text{Fe}+\text{Co}$, $B_{\text{eq}}=(8\pi^2/3)[U_{33}+4(U_{11}+U_{22}-U_{12})/3]$. An asterisk indicates that only isotropic factors were refined.

Atom	Site	x/a	y/b	z/c	SOF	$B_{\text{eq}}, B_{\text{iso}}^*$
Ba	2d	2/3	1/3	1/4	1	1.08(3)
M1	2a	0	0	0	1	0.76(5)*
M2	4e(1/2)	0	0	0.2372(1)	0.5	0.63(9)
M3	4f ₁	1/3	2/3	0.026 45(7)	1	0.84(4)*
M4	4f ₂	1/3	2/3	0.188 79(8)	0.520(3)	0.77(4)
Sn4					0.479	
M5	12k	0.1676(3)	0.3353	-0.105 88(3)	0.945(3)	1.01(2)*
Sn5					0.055	
O1	4e	0	0	0.1497(3)	1	1.01(9)*
O2	4f	1/3	2/3	-0.0551(3)	1	1.17(9)*
O3	6h	0.1830(5)	0.3661	1/4	1	0.98(9)*
O4	12k	0.1551(3)	0.3102	0.0523(2)	1	1.01(6)*
O5	12k	0.5050(4)	1.0100	0.1492(2)	1	1.04(6)*

evident the preference of Sn for the 4f₂ sites at the face-sharing octahedra, and to a much lower extent, for the 12k sites at the edge sharing octahedra lying on the R-S interphase. The final agreement factors were $R=3.20\%$ and $wR=3.00\%$. After the refinement, Fourier difference peaks remained along the line $\frac{1}{3}, \frac{2}{3}, z$ joining 4f₂ sites at $z/c=0.14, 0.36 \rightarrow 1.00 \text{ e \AA}^{-3}$; $z/c=0.19, 0.31 \rightarrow -0.72 \text{ e \AA}^{-3}$ [(M,Sn)4 main position]; $z/c=0.22, 0.28 \rightarrow 0.22 \text{ e \AA}^{-3}$, and $z/c=0.25 \rightarrow -0.84 \text{ e \AA}^{-3}$, which were attributed to the effect of the disorder and electrostatic repulsion associated to the Sn population in the face-sharing octahedra.

C. Magnetization

The magnetic study was performed using a single crystal obtained in the first experiment, with average $x=0.9$, since this composition is close to those that are interesting for magnetic recording (in polycrystalline samples). Isothermal magnetization measurements were performed with a superconducting quantum interference device (SQUID) magnetometer (Quantum Design) in fields up to 5.5 T at $T=5$ and 330 K. The external field was either oriented parallel or perpendicular to the c axis (the easy magnetization direction).

III. RESULTS AND DISCUSSION

A. Structure

Structural results are summarized in Table I, Fig. 1 shows a drawing of the content of the unit cell, and Table II shows the cation-oxygen distances within each coordination polyhedron. Assuming the formal stoichiometry of $\text{BaFe}_{12-2x}\text{Co}_x\text{Sn}_x\text{O}_{19}$, the refined Sn site occupation factors gave rise to $x=1.28$. This result is in good agreement with the EDAX composition taking into account the small compositional dispersion within the crystals obtained in one single batch.

In accordance with Sn⁴⁺ containing II-IV spinels²⁰ we have found that in the present compound Sn only enters octahedral sites. However, a pronounced occupational hierarchy is established, which follows in order of preference $4f_2 \gg 12k$ and the 2a octahedra (spinel block) are free of

any Sn at all. This pronounced occupational hierarchy was suggested in a previous work for powder samples with composition $x < 0.5$, from isothermal magnetization, $M(H)$, curves at 4.2 K with applied fields up to 20 T.²¹ Further substitution (up to $x \sim 1$) induced a strong spin noncolinearity, which precluded any interpretation about cation distribution. Therefore, our present study indicates that the occupancy trend of Sn⁴⁺ cations does not change significantly in the substitution range $0 < x < 1.28$.

The high Sn⁴⁺ concentration in the face-sharing 4f₂ octahedra generates a strong electrostatic repulsion. Accordingly, the mean (M,Sn)4-(M,Sn)4 distance, 2.875(4) Å, is larger than the corresponding one in $\text{BaFe}_{12}\text{O}_{19}$, 2.768(1) Å,⁴ so that the cations are shifted along the c -axis direction towards the neighboring empty octahedral sites.

TABLE II. Important distances (Å) in $\text{BaFe}_{12-2x}\text{Sn}_x\text{Co}_x\text{O}_{19}$ ($x=1.28$).

BaI cubooctahedron (R block)	
Ba-O3:	2.972(1) × 6
Ba-O5:	2.893(4) × 6
M1 octahedron (S block)	
M1-O4:	2.013(4) × 6
M2 dipyrmaid (R block)	
M2-O1:	2.055(8) × 1
	2.654(8) × 1
M2-O3:	1.905(5) × 3
O3-O3:	3.259(5)
O3-O1:	3.015(5)
M2-M2:	0.601(4)
M3 tetrahedron (S block)	
M3-O2:	1.914(8) × 1
M3-O4:	1.930(3) × 3
(M,Sn)4 octahedron (R block)	
(M,Sn)4-O3:	2.110(4) × 3
(M,Sn)4-O5:	1.995(4) × 3
(M,Sn)5 octahedron (R-S interphase)	
(M,Sn)5-O1:	2.007(4) × 1
(M,Sn)5-O2:	2.079(5) × 1
(M,Sn)5-O4:	2.085(4) × 2
(M,Sn)5-O5:	1.966(4) × 2

TABLE III. Bond strengths and apparent valencies in $\text{BaFe}_{12-x}\text{Co}_x\text{Sn}_x\text{O}_{19}$ ($x=1.28$), assuming $M=\text{Fe}^{3+}$.

	O1	O2	O3	O4	O5	Σ_{calc}
Ba			0.156×6		0.193×6	2.09
M1				0.503×6		3.02
M2	0.449×1	0.674×3				2.47
M3		0.659×1		0.630×3		2.55
(M,Sn)4			0.453×3		0.618×3	3.21
(M,Sn)5	0.521×1	0.429×1		0.422×2	0.582×2	2.96

In consequence, the coordination polyhedra are noticeably distorted: The edges on the shared face are much shorter [$2.675(5) \text{ \AA}$] than the edges lying on the adjacent O_4 layers [$3.056(4) \text{ \AA}$], so that the surface area of the shared face is reduced in order to screen the two neighboring Sn^{4+} cations.

A similar Sn occupational hierarchy has been observed in other related compounds.²² A recent study of the *K*-type ferrite $\text{Ba}_2\text{Fe}_{10}\text{Sn}_2\text{CoO}_{22}$,²³ described by a ...*QS*... block sequence, indicated the inability of Sn^{4+} to occupy the *S* block octahedra. We have also observed a similar hierarchy within the *R* block in the *R*-type compound $\text{BaFe}_{4-2x}\text{Sn}_{2+x}\text{Co}_x\text{O}_{11}$ ($x=1.32$),²⁴ where selective dilution in the face sharing octahedra amounts to 100%, canceling long-range magnetic order.

In order to get some insight into the possible Co^{2+} location, apparent valencies¹⁴ were calculated on the basis $M=\text{Fe}^{3+}$ and the refined composition $M_{1-p}\text{Sn}_p$ in each site, *p* being the Sn site occupation factor. For this purpose the following expression was used:¹⁴

$$\Sigma_{\text{calc}} = \sum_j \exp\left(\frac{r_0 - d_{ij}}{0.37}\right), \quad (1)$$

where r_0 is a constant characteristic of each species participating in the cation-anion bond, and the d_{ij} 's are the measured bond distances between the *i*th cation and *j*th oxygen.²⁵ These results are summarized in Table III. In the present compound these values are more significant when disorder is limited to Fe^{3+} and Co^{2+} . Among the two different blocks described so far, the *S* (spinel-like) block is the best suited to this situation since no Sn^{4+} was detected. Looking at Table III, the main conclusions may be summarized as follows: (i) We found that the apparent valence calculated for the M1 cation, located in the *2a* site, $\Sigma_{\text{calc}}=3.02$ is representative of a full Fe^{3+} occupancy, in good agreement with neutron powder diffraction studies, in which we found that no Co^{2+} cations enter the *2a* site up to $x=1.0$ in both Co-Ti and Co-Sn powder samples.^{10,12,13} (ii) The M3 cation in the $4f_1$ tetrahedra shows an anomalous low value which may be an indication of the preferential occupation by Co^{2+} cations, also in good agreement with previous neutron powder results.^{12,13} It is worth noticing that the Co^{2+} content in the $4f_1$ sites amounts to 40% of the whole Co^{2+} quantity when $x=0.2$.¹² The same trend has been observed in the *Y*-type structure.²⁶ This observation contrasts with the previous assumptions made about Co^{2+} distributions in hexagonal ferrites from the dependence of the saturation magnetization on the substi-

tion rate or from microwave ferromagnetic resonance measurements,²⁷ which stated the strict preference of Co^{2+} cations for octahedral sites. (iii) The Σ_{calc} values calculated for $4f_2$ and $12k$ sites [(M,Sn)4 and (M,Sn)5 cations, respectively] are slightly lower than the expected ones for $(\text{Fe}_{0.520(3)}\text{Sn}_{0.480})4$ and $(\text{Fe}_{0.945(3)}\text{Sn}_{0.055})5$ compositions, respectively. However, disorder and in particular the strong distortion of the coordination polyhedron of (M,Sn)4 cations may reduce the reliability of apparent valencies.¹⁴ As will be shown in the following subsection, magnetic measurements point to a non-negligible amount of Co^{2+} cations occupying the $12k$ octahedra.

Of particular interest is the nature of the cation located in the trigonal dipyramidal environment. Obradors *et al.*⁴ showed that in $\text{BaFe}_{12}\text{O}_{19}$, the dipyramidal Fe^{3+} cations display a dynamical disorder between two pseudotetrahedral sites separated by $0.340(1) \text{ \AA}$. A characteristic structural consequence of this situation is the pronounced axial compression of the dipyramid, so that the shared edge between the two linked tetrahedra (site 2, see Fig. 1) is large allowing the diffusion of Fe^{3+} through the equator of the dipyramid. However, in our case the distance between the two equilibrium positions is much larger, $d_{\text{M2-M2}}=0.601(4) \text{ \AA}$, indicating that the cation is more likely to have fourfold coordination being statically disordered between both adjacent tetrahedra. Further work is needed to elucidate this extreme. Our rms thermal amplitude parallel and perpendicular to the *c* axis, 0.15 and 0.10 \AA , respectively, are also somewhat higher than in the pure compound,⁴ 0.09 \AA (parallel) and 0.08 \AA (perpendicular), especially along the *c* axis, and this could be the signature of some degree of Fe^{3+} substitution by Co^{2+} . This assumption is consistent with the low value of $\Sigma_{\text{calc}}=2.47$ of this site. Taking into account the difference in size between Co^{2+} and Fe^{3+} cations,²⁸ further evidence for the presence of Co^{2+} cations occupying these sites may be achieved by comparing the volumes of the dipyramids in the pure and substituted compounds. These volumes are 6.8 \AA^3 for $\text{BaFe}_{12}\text{O}_{19}$ (according to the data of Ref. 4) and 7.2 \AA^3 for our present single crystal. Regardless of the dynamic or static nature of these sites, this observation supports the presence of Co^{2+} cations, in agreement with single-crystal neutron-diffraction results by Kaldova *et al.*²⁹ on $\text{BaFe}_8\text{Co}_2\text{Ti}_2\text{O}_{19}$.

B. Magnetic properties

The magnetic characterization of the $\text{BaFe}_{12-2x}\text{Co}_x\text{Sn}_x\text{O}_{19}$ has been carried out by using a single

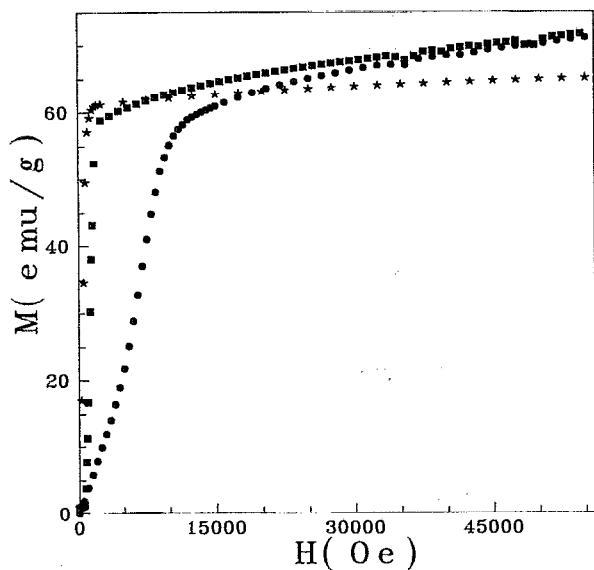


FIG. 2. Isothermal magnetization curves with the applied field parallel to the easy direction of magnetization (c axis) (\square : $T=5$ K; $*$: $T=300$ K) and perpendicular to it (\circ : $T=5$ K).

crystal with composition $x=0.9$ in a SQUID magnetometer. We have studied the magnetization process with the external applied field parallel and perpendicular to the hexagonal c axis.

In Fig. 2 we show the magnetization curves with the applied field in both directions. It is evident from the figure that the easy direction of magnetization is parallel to the c axis and thus the compound still exhibits uniaxial anisotropy for this composition. Nevertheless, we observe that the magnetization curve with the applied field perpendicular to the c axis shows an upturn around $H \sim 6$ kOe that becomes smoother as temperature increases and disappears at $T \sim 150$ K. To determine the nature of this behavior we have performed a complete study of the magnetization process in the perpendicular direction as a function of temperature.

The total magnetic energy may be represented by the relation

$$E_m = K_1 \sin^2 \vartheta + K_2 \sin^4 \vartheta + K_3 \sin^6 \vartheta - M_s H \sin \vartheta + \frac{1}{2} (4\pi/3) M_s^2 \sin^2 \vartheta, \quad (2)$$

where ϑ is the angle between M and the hexagonal c axis, K_1 , K_2 , and K_3 are the anisotropy constants, and M_s is the saturation magnetization.

The minimization of E_m with respect to the angle ϑ gives³⁰

$$\frac{H}{M} = \left(\frac{2K_1}{M_s^2} + \frac{4\pi}{3} \right) + \frac{4K_2}{M_s^4} M^2 + \frac{6K_3}{M_s^6} M^4. \quad (3)$$

In Fig. 3 we show the typical H/M vs M^2 curves; from these curves one observes that K_3 should be very small in front of K_1 and K_2 whose values may be obtained from the

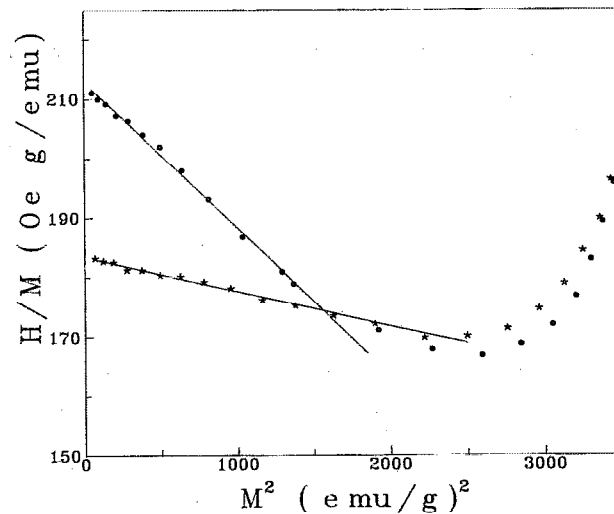


FIG. 3. Curves of H/M vs M^2 showing the zone of linear dependence from which the anisotropy constants K_1 and K_2 may be determined in agreement with Eq. (3). (\circ : $T=10$ K; $*$: $T=70$ K).

intercept in the y axis and the slope, respectively. The results obtained in this way are shown in Fig. 4 going from $T=5$ to 250 K.

We observe from the figure that the second anisotropy constant K_2 decreases faster than K_1 and becomes very small around $T \sim 150$ K. As we have pointed out above, the upturn observed in the magnetization curve when the applied field is perpendicular to the c axis has a parallel thermal dependence and disappears around $T \sim 150$ K, so we conclude that this anomaly on the magnetization curve is due to the competition of different anisotropy directions. From the sign ($K_1 > 0$) and the ratio $|K_1/K_2| > 2$ it is possible to conclude that the system has uniaxial anisotropy and the easy direction of magnetization is parallel to

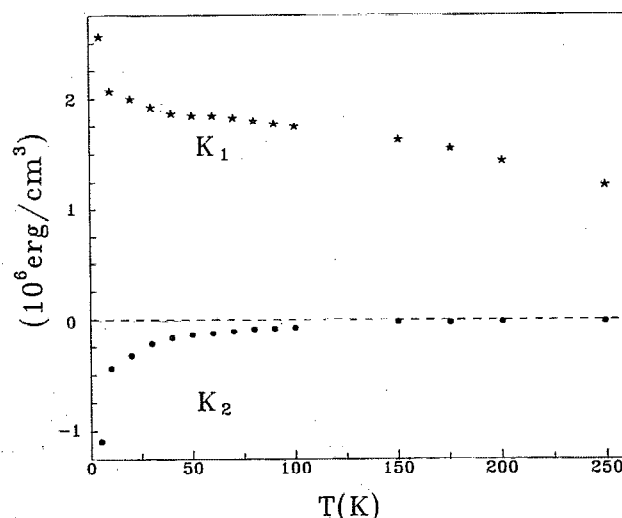


FIG. 4. Thermal dependence of the anisotropy constants K_1 and K_2 determined by using Eq. (3).

the c axis.³¹ On the other hand, in the high-field range the isothermal magnetization curves can be described by

$$M = M_s + \chi_d H, \quad (4)$$

χ_d being the high-field differential susceptibility. In both cases (the applied field H parallel and perpendicular to the hexagonal c axis) a high value of $\chi_d \sim 2 \times 10^{-4}$ emu/g is found at $T \sim 5$ K, a value that is considerably higher than that corresponding to the Co-Ti system, thus pointing out the existence of a stronger noncolinear magnetic structure in the Co-Sn doping scheme in good agreement with previous results obtained in powder samples.^{11,12}

The origin of this noncolinearity of the magnetic structure may be attributed to the preferential location of the Sn^{4+} cations in the $4f_2$ sites, destroying $12k-4f_2$ and $4f_2-4f_2$ superexchange paths, lowering in such a way the isotropic exchange energy that is responsible for the colinear uniaxial magnetic structure in the nondoped ($x=0$) compound.⁵ As the Sn^{4+} content increases, more superexchange paths are broken and second-order energy terms such as the antisymmetric interaction³² or magnetocrystalline anisotropy start to play their role, and noncolinear structures may appear as is the case of doped ferrites.

It is observed that, among the five metallic sublattices, the octahedral $12k$ sites are where competing interactions are stronger,⁷ and consequently, the stabilization energy is the lowest. So $12k$ sites are very sensitive to nonmagnetic substitution in their nearest-neighboring sites, namely $4f_1$ and $4f_2$. A similar effect is also observed in the Co-Ti substitution scheme.^{10,13}

It is worth mentioning that saturation is not reached at $T=5$ K in any of the directions of the external applied field up to 55 kOe. We also show in Fig. 2 a magnetization curve with the external applied field parallel to the c axis at $T=330$ K. Even at this temperature a considerable value of χ_d is found ($\chi_d \sim 5.2 \times 10^{-5}$ emu/g) signaling that some degree of noncolinearity still exists in the magnetic structure.

A detail of the magnetization curve in the low-field range at $T=5$ K is shown in Fig. 5. A coercive field H_c of around 900 Oe and a remanent magnetization $M_r \sim 40$ emu/g is observed with the applied field parallel to the c axis. A very similar value of H_c is obtained in the perpendicular direction but with a very small value of M_r (~ 3 emu/g).

Regarding the technological applicability of the Co-Sn doping scheme as a material suitable for magnetic recording, the M_s value at room temperature is around 10% lower than that for the nondoped compound ($H_s \sim 68$ emu/g for $\text{BaFe}_{12}\text{O}_{19}$)² and the anisotropy constant K_1 reduces almost to half ($K_1 = 4.4 \times 10^6$ erg/cm³ for $\text{BaFe}_{12}\text{O}_{19}$ at $T=4.2$ K).³³

When comparing the above results with those corresponding to the Co-Ti system we observe that K_1 is slightly smaller ($K_1 \sim 2.8 \times 10^6$ erg/cm³ for the same doping rate for Co-Ti,¹⁰ in front of 2.6×10^6 erg/cm³ for Co-Sn) and the saturation magnetization is considerably smaller (around 20%) as well as the coercive field^{11,34} while the differential susceptibility is clearly higher. The decrease of

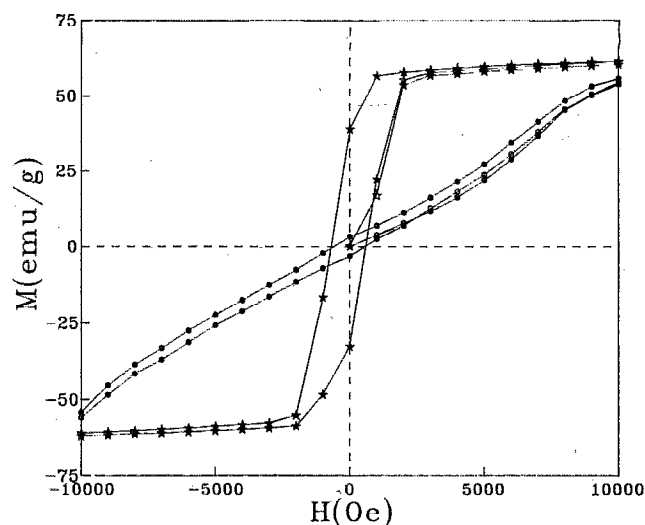


FIG. 5. Low-field region of the magnetization curve showing the hysteresis loops with the external applied field parallel (*) and perpendicular (O) to the c axis.

the magnetic anisotropy in both doped systems in front of the nondoped compound is due to the partial cancelation of the uniaxial magnetocrystalline anisotropy of the pure compound by means of the planarlike ($K_1 < 0$) single-ion anisotropy contribution of Co^{2+} ions occupying $12k$ sites.³⁵ The differences between Co-Ti and Co-Sn systems reflect the fact that a larger quantity of Co^{2+} ions occupy tetrahedral sites in the former case, thus being ineffective in the reduction of the intrinsic uniaxial magnetic anisotropy. This different occupation of tetrahedral sites by Co^{2+} together with the strong preference of Sn^{4+} ions for $4f_2$ octahedral sites lies at the origin of the higher effectiveness of the Co-Sn doping scheme in lowering the uniaxial anisotropy and coercive field of $\text{BaFe}_{12}\text{O}_{19}$.

Referring to the microscopic magnetic structure we cannot get information from our macroscopic measurements. Furthermore, the lack of the magnetic phase diagram for the Co-Sn doping scheme makes it more difficult. Having in mind the preliminary phase diagram for the Co-Ti substitution scheme³⁶ and our results for powder samples,^{10,21} it seems to indicate that the colinearity of the magnetic structure is lost for doping rates above $x=0.5$ for Co-Sn and $x=0.7$ for Co-Ti systems. The magnetic ground state is no longer that of a colinear ferrimagnet but that of a disordered ferrimagnet. A neutron-diffraction study will be necessary to determine the microscopic magnetic structure as a function of doping rate.

ACKNOWLEDGMENT

This work has been supported by the CICYT, Project No. MAT88-0259.

¹M. P. Sharrock, IEEE Trans. Magn. **MAG-25**, 4374 (1989); M. H. Kryder, J. Magn. Magn. Mater. **83**, 1 (1990); P. Gerard, E. Lacroix, G. Marest, M. Dupuy, G. Rolland, and B. Blanchard, J. Magn. Magn. Mater. **83**, 13 (1990).

²H. Kojima, in *Ferromagnetic Materials*, edited by E. P. Wohlfarth (North-Holland, Amsterdam, 1982), Vol. 3.

- ³V. Adelsköd, Ark. Kem. Mineralog. Geol. Ser. A 12, 1 (1938).
- ⁴X. Obradors, A. Collomb, M. Pernet, D. Samaras, and J. C. Joubert, J. Solid State Chem. 56, 171 (1985).
- ⁵E. W. Gorter, Proc. IEEE 104B, 225 (1957).
- ⁶G. Albanese, J. Phys. (Paris) Colloq. 38, C1-85 (1977).
- ⁷A. Isalgué, A. Labarta, J. Tejada, and X. Obradors, Appl. Phys. A 38, 3063 (1985).
- ⁸X. Batlle, A. Labarta, B. Martínez, X. Obradors, M. V. Cabañas, and M. Vallet, J. Appl. Phys. 70, 6172 (1991).
- ⁹H. Hübner, Angew. Chem. Int. Ed. Engl. 21, 270 (1982).
- ¹⁰X. Batlle, X. Obradors, J. Rodríguez-Carvajal, M. Pernet, M. V. Cabañas, and M. Vallet, J. Appl. Phys. 70, 1614 (1991) and references cited therein.
- ¹¹M. Pernet, X. Obradors, M. Vallet, T. Hernández, and P. Germi, IEEE Trans. Magn. MAG-24, 1898 (1988).
- ¹²X. Batlle, J. Rodríguez, X. Obradors, M. Pernet, M. Vallet, and J. Fontcuberta, J. Phys. (Paris) Colloq. 49, C8-939 (1988).
- ¹³X. Batlle, M. V. Cabañas, X. Obradors, M. Vallet, and J. Rodríguez, in *Spanish Contribution to Neutron Scattering Techniques*, edited by J. C. Gómez Sal, J. M. Baramdarían, and F. Rodríguez González (University of Cantabria, Cantabria, 1992), pp. 47-57.
- ¹⁴M. O'Keeffe, Structure Bonding 71, 161 (1989).
- ¹⁵F. Sandiumenge, S. Galí, and R. Rodríguez-Clemente, J. Cryst. Growth 110, 617 (1991).
- ¹⁶F. Sandiumenge, S. Veintemillas-Verdaguer, R. Rodríguez-Clemente, and S. Galí, J. Cryst. Growth 121, 247 (1992).
- ¹⁷ZAF-4/FLS (Link systems, Ltd.) system for the correction of atomic number, fluorescence, and absorption in energy-dispersive x ray (EDX) analysis.
- ¹⁸*International Tables for X-Ray Crystallography* (Kynoch, Birmingham, 1974), Vol. 2, p. 302.
- ¹⁹G. M. Sheldrick, SHELX-76 Program for Crystal Structure Determination, University of Cambridge, England, 1976.
- ²⁰N. C. Greenwood, *Cristales Iónicos, Defectos Reticulares y No Estequiometría* (Ed. Alhambra, Madrid, 1970).
- ²¹X. Batlle, Ph.D. thesis, University of Barcelona, 1990.
- ²²F. Sandiumenge, Ph.D. thesis, University of Barcelona, 1991.
- ²³F. Sandiumenge, S. Galí, R. Rodríguez-Clemente, X. Batlle, and X. Obradors, J. Solid State Chem. 92, 213 (1991).
- ²⁴B. Martínez, F. Sandiumenge, S. Galí, X. Obradors, and R. Rodríguez-Clemente, Solid State Commun. 83-8, 649 (1992); F. Sandiumenge, S. Galí, and R. Rodríguez-Clemente, Mater. Res. Bull. 27, 417 (1992).
- ²⁵I. D. Brown, and Altermatt, Acta Cryst. B 41, 244 (1985).
- ²⁶A. Collomb, M. A. Hadj-Farhat, and J. C. Joubert, Mater. Res. Bull. 24, 459 (1989).
- ²⁷D. J. Bitetto, J. Appl. Phys. 35, 3482 (1964).
- ²⁸D. Shannon, Acta Cryst. A 32, 1751 (1976).
- ²⁹L. Kaldova, M. Dlouhá, S. Vratislav, and Z. Jiráček, J. Magn. Magn. Mater. 87, 243 (1990).
- ³⁰W. Sucksmith and F. R. S. Thompson, Proc. R. Soc. London xx, 225 (1954); D. Le Roux, thesis, Université Scientifique Technologique et Médicale de Grenoble, Grenoble, France, 1986.
- ³¹A. Herpin, *Théorie du Magnétisme* (P.U.F., Paris, 1967).
- ³²T. Moriya, Phys. Rev. 120, 2 (1960).
- ³³J. Smit and H. P. J. Wijn, *Ferrites* (Philips Technical Library, Eindhoven, 1959).
- ³⁴O. Kubo, T. Ido, and M. Yokozama, IEEE Trans. Magn. MAG-18, 1122 (1982).
- ³⁵J. C. Slonczewski, Phys. Rev. 110, 1341 (1958); F. Bolzoni and L. Pareti, J. Magn. Magn. Mater. 35, 135 (1984); F. Chou, X. Feng, J. Li, and Y. Lin, J. Appl. Phys. 61, 3381 (1987).
- ³⁶R. A. Sadykov, O. P. Alesko-Ozhevskii, and N. A. Arsen'ev, Sov. Phys. Solid State 23, 1090 (1981).